Nuclear Engineering and Technology 53 (2021) 967–973

Contents lists available at ScienceDirect

Nuclear Engineering and Technology

journal homepage: www.elsevier.com/locate/net

Original Article

Methodology of seismic-response-correlation-coefficient calculation for seismic probabilistic safety assessment of multi-unit nuclear power plants

Seunghyun Eem [a], In-Kil Choi [b], Beomjoo Yang [c], Shinyoung Kwag [d, *]

[a] Department of Conversion and Fusion System Engineering, Major in Plant System Engineering, Kyungpook National University, South Korea
[b] Structural Safety & Prognosis Research Division, Korea Atomic Energy Research Institute, South Korea
[c] School of Civil Engineering, Chungbuk National University, South Korea
[d] Department of Civil and Environmental Engineering, Hanbat National University, South Korea

ARTICLE INFO

Article history:
Received 23 April 2020
Received in revised form
16 July 2020
Accepted 23 July 2020
Available online 1 August 2020

Keywords:
Seismic PSA
Seismic correlation
Incoherence function
Seismic-response analysis
Multi-unit

ABSTRACT

In 2011, an earthquake and subsequent tsunami hit the Fukushima Daiichi Nuclear Power Plant, causing simultaneous accidents in several reactors. This accident shows us that if there are several reactors on site, the seismic risk to multiple units is important to consider, in addition to that to single units in isolation. When a seismic event occurs, a seismic–failure correlation exists between the nuclear power plant's structures, systems, and components (SSCs) due to their seismic-response and seismic-capacity correlations. Therefore, it is necessary to evaluate the multi-unit seismic risk by considering the SSCs' seismic-failure-correlation effect. In this study, a methodology is proposed to obtain the seismic-response-correlation coefficient between SSCs to calculate the risk to multi-unit facilities. This coefficient is calculated from a probabilistic multi-unit seismic-response analysis. The seismic-response and seismic-failure-correlation coefficients of the emergency diesel generators installed within the units are successfully derived via the proposed method. In addition, the distribution of the seismic-response-correlation coefficient was observed as a function of the distance between SSCs of various dynamic characteristics. It is demonstrated that the proposed methodology can reasonably derive the seismic-response-correlation coefficient between SSCs, which is the input data for multi-unit seismic probabilistic safety assessment.

1. Introduction

In March 2011, the accident at the Fukushima Daiichi Nuclear Power Plant highlighted the importance of considering the risks to multiple-reactor facilities and generated huge interest in probabilistic seismic safety assessment of multi-unit risk. Most probabilistic safety assessments (PSAs) are based on considering only a single unit in isolation and are not able to fully account for all possible accident sequences [1]. A PSA of multi-unit risk should be able to evaluate more such scenarios. Research has been conducted on multi-unit risk by many researchers [2–7]. In Korea, several nuclear power plants contain multiple reactors, and efforts are being made to perform multi-unit PSA (MUPSA) with inter-unit common-cause-failure modeling [4]. However, seismic events differ from internal events because they are influenced by spatial in variation in where the power plant's structures, systems, and components (SSCs) are located.

The seismic safety of nuclear power plants is generally evaluated through PSA. The probability of structural and component failure due to earthquakes is represented by a fragility curve, and it is assumed that each failure occurs independent or fully correlated. However, the seismic response and capacity are correlated between SSCs, and thus, failure probability is also correlated between them. This failure correlation will affect the assessed seismic-risk value, which is considered the failure correlation as independently. The seismic correlation can increase or decrease the seismic risk of the system. In other words, the failure correlation of SSCs should be considered in seismic PSA [8].

Seismic PSA of nuclear power plants with consideration of failure correlation has been conducted mainly in studies of single-

* Corresponding author.
E-mail addresses: eemsh@knu.ac.kr (S. Eem), cik@kaeri.re.kr (I.-K. Choi), byang@cbnu.ac.kr (B. Yang), skwag@hanbat.ac.kr (S. Kwag).

https://doi.org/10.1016/j.net.2020.07.032

unit risk. The importance of seismic-failure correlation in this context was addressed in the WASH-1400 study and in the Seismic Safety Margins Research Program (SSMRP) study conducted by the Lawrence Livermore National Laboratory in the United States [9]. In the SSMRP study, a multi-integration method was proposed to perform a seismic PSA considering failure correlation, but the correlation between SSCs was mainly studied only under completely independent or completely dependent conditions [10]. Mankamo suggested a method for calculating the probability of simultaneous failure by expressing its probability as a function of multipliers through the Mankamo model. The present author proposed a method for evaluating seismic risk with consideration of the seismic-failure-correlation determined by BDD and MCS [11]; however, there is no consensus method for obtaining the seismic-failure correlation. Hence, industry usually considers only complete independence or complete dependence of the SSCs [10].

The SSMRP study proposed a method to find the seismic-failure-correlation coefficient between SSCs based on the seismic-response and seismic-capacity-correlation coefficients. The latter can be obtained through tests and the former can be derived through seismic-response analysis [12]. Bohn proposed rules for assigning response correlation, for which the seismic-response-correlation coefficient between SSCs is found via an empirical approach [13]. Ebisawa proposed a method for obtaining the seismic-response-correlation coefficient via seismic-response analysis [2].

In the present study, a methodology is proposed to calculate the seismic-response-correlation coefficients of SSCs installed at different locations through seismic-response analysis. A probabilistic seismic-response analysis was performed to calculate the seismic-response-correlation coefficient for the emergency diesel generators installed in various units. Based on the analytical results, the seismic-response and the seismic-failure-correlation coefficients of the emergency diesel generators were successfully obtained. In addition, the seismic-response-correlation-coefficient distribution was investigated as a function of the distance between SSCs.

2. Materials and methods

SSCs at a nuclear power plant will exhibit seismic responses when a seismic event occurs, and because they experience the same input ground motion, these responses may be relatively similar. Due to this similarity, the SSCs' failure probabilities are correlated, and this correlation should be considered when evaluating the nuclear power plant's seismic safety. Seismic-failure-correlation coefficients are needed to consider this effect in PSAs. In the SSMRP study, it was suggested that this coefficient could be calculated as

$$\rho_{12} = \frac{\beta_{R1}\beta_{R2}}{\sqrt{\beta_{R1}^2+\beta_{C1}^2}\sqrt{\beta_{R2}^2+\beta_{C2}^2}}\rho_{R1R2} + \frac{\beta_{C1}\beta_{C2}}{\sqrt{\beta_{R1}^2+\beta_{C1}^2}\sqrt{\beta_{R2}^2+\beta_{C2}^2}}\rho_{C1C2}, \quad (1)$$

where ρ_{12} is the failure-correlation coefficient of components 1 and 2, β_{R1} and β_{R2} are the standard deviations of the logarithms of the responses of components 1 and 2, β_{C1} and β_{C2} are the standard deviations of the logarithms of the capacities of components 1 and 2, ρ_{R1R2} is the response-correlation coefficient of components 1 and 2, and ρ_{C1C2} is the capacity-correlation coefficient of components 1 and 2.

As can be seen from Eq. (1), to calculate the seismic-failure-correlation coefficient between SSCs, it is necessary to know the seismic-response and seismic-capacity-correlation coefficients. The latter can be derived from the SSC's seismic test data, and the former can be calculated through seismic-response analysis [14]. In the SSMRP study, the seismic-failure-correlation coefficient between SSCs was used to evaluate single-unit risk; however, Eq. (1) can also be used for multi-unit risk.

Probabilistic seismic-response analysis should be performed to obtain the seismic-response-correlation coefficient between SSCs. This coefficient can be calculated from the seismic-response distribution of SSCs via Eq.(2) [2,14]:

$$\rho_{Ri,Rj} = \frac{Cov(X_i(a), X_j(a))}{\sigma_i \sigma_j}, \quad (2)$$

where X_i(a) and X_j(a) are random variables for SSC responses i and j, respectively, σ_i and σ_j are standard deviations of X_i(a) and X_j(a), and Cov(X_i(a),X_j(a)) is the covariance of X_i(a) and X_j(a).

Fig. 1 presents a schematic diagram of the similarity of seismic-wave signals for multi-unit risk. The seismic-wave signals from the two points, A and B, will be similar as they have the same source, a similar path, and similar soil conditions. Moreover, as the distance between A and B increases, the similarity of the seismic-wave signals will decrease. The seismic-response distribution of the SSCs in a single-unit is due to the uncertainty of the SSCs and the randomness of the earthquakes; however, the seismic-response distribution for multi-unit facilities should additionally consider the spatial variation due to the SSCs' installation location. The randomness of the earthquake and the uncertainty of the SSCs can be considered by probabilistic seismic-response analysis, which is used for single-unit risk. Additionally, for multi-unit risk, each unit should have a different seismic ground motion for each seismic event. In this study, a methodology is proposed to generate the input earthquake for each unit using a seismic-motion-coherency function to calculate the seismic-response-correlation coefficient between SSCs for multi-unit risk.

The ordinary coherence function is defined as the measure of the causal relationship between two signals with the presence of other signals. Mathematically, the coherency $\gamma_{ij}(\omega)$ is expressed as Eq. (3):

$$\gamma_{i,j}{}^2 = \frac{|S_{ij}(\omega)|^2}{S_{ii}(\omega)S_{jj}(\omega)}, \quad (3)$$

where $S_{ij}(\omega)$ is the smoothed cross-spectrum for signals i and j. The coherence varies in the interval $0 \le \gamma_{ij}^2 \le 1$; if coherence is equal to 1, it means that the signals are perfectly correlated or linearly related; if coherence is equal 0, they are totally uncorrelated. The spatial variability of ground-motion waveforms can be quantified by coherence. There are local wave-scattering and wave-passage effects for seismic-motion coherence, indicating spatial variation. In seismic-motion coherence, spatial correlation decreases with frequency and separation distance [15]. A seismic-motion-coherence function is commonly used in soil-structure-interaction analysis. Several seismic-motion-coherence-function models have been proposed for considering spatial variability [16–22].

The seismic-motion-coherence function proposed by Abrahamson is an empirical model and the most representative of such functions [15,16]. It is based on evaluating the ground motions from the extensive databases taken by the SMART 1 dense array in Lotung, Taiwan [23]. This function is presented in Eq. (4):

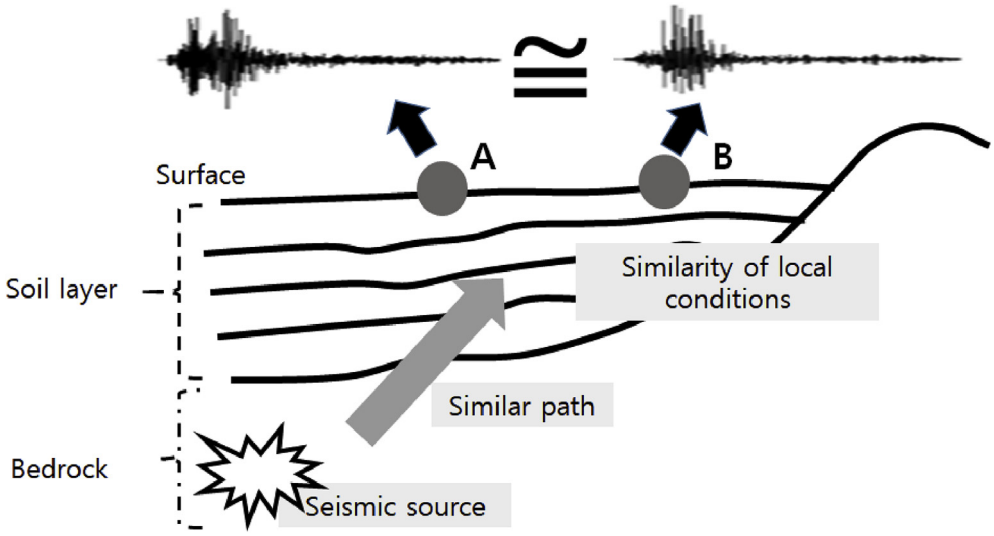

Fig. 1. A schematic diagram of the similarity of the seismic-wave signals.

$$\gamma(f,\xi)=\left[1+\left(\frac{f\ Tanh(a_3\xi)}{a_1 f_c(\xi)}\right)^{n1}\right]^{-1/2}\left[1+\left(\frac{f\ Tanh(a_3\xi)}{a_2 f_c(\xi)}\right)^{n2(\xi)}\right]^{-1/2}, \tag{4}$$

where f is the frequency [Hz] and ξ is the separation distance [m]. Tables 1 and 2 give the horizontal and vertical components.

Fig. 2 shows Abrahamson's seismic-motion-incoherence function for distances between SSCs of 100 m, 200 m, and 300 m. The seismic-motion-incoherence function decreases as frequency increases, and has a generally smaller amplitude for higher separations.

This function expresses the similarity of the earthquake inputs occurring at any two points. Therefore, to obtain multi-unit risk, the similarity of the earthquake inputs at the positions of each unit are considered. Using these generated earthquakes, the seismic-response distribution of the SSCs can be calculated from the probabilistic seismic-response analysis, and the result can be applied to Eq. (2) to obtain the seismic-response-correlation coefficient between SSCs.

When considering seismic risk for two or more units, the generated earthquake must satisfy the seismic-motion-coherence function between each pair of units. In other words, 3 seismic-motion-coherence functions must be satisfied for 3 units, and 6 seismic-motion-coherence functions must be satisfied for 4 units.

3. Application

In this section, the seismic-motion-coherence function is used to calculate the seismic-response-correlation coefficient between SSCs in an example. The example is that of finding the seismic-response-correlation coefficient between emergency diesel generators located in separate auxiliary buildings; a schematic diagram is shown in Fig. 3. Twin units are situated 100 m apart on the same site. The site was assumed to be made of solid rock, and soil-structure interaction was not considered. Because the units are close together, they have the same response spectrum, which is taken from the NRC's Regulatory Guide 1.60 (pga: 0.3 g). The uncertainty of the structure properties itself is considered, but the property's correlation between the structures is considered as independent.

First, the input earthquakes to the two units satisfy the

Table 1
Coherence-model coefficients for the horizontal components [15].

Coefficient	Horizontal Components
a_1	1.647
a_2	1.01
a_3	0.4
n_1	7.02
n_2	$5.1-0.51\ \ln(\xi+10)$
$f_c(\xi)$	$-1.886+2.221\ \ln\left(\frac{4000}{\xi+1}+1.5\right)$

Table 2
Coherence-model coefficients for the vertical components [15].

Coefficient	Vertical Components
a_1	3.15
a_2	1.0
a_3	0.4
n_1	4.95
n_2	1.685
$f_c(\xi)$	$\exp(2.43-0.025\ \ln(\xi+1)-0.048[\ln(\xi+1)]^2$

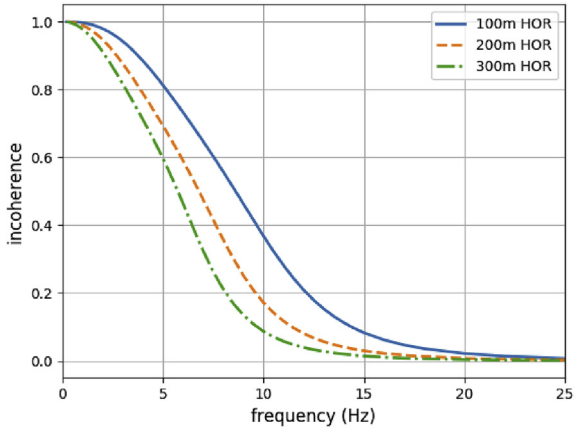

Fig. 2. Abrahamson's seismic-motion-incoherence function.

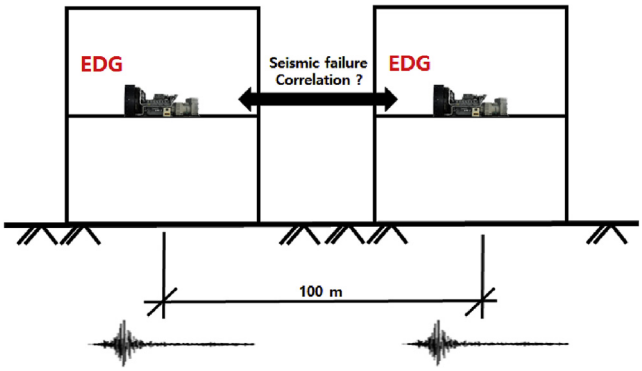

Fig. 3. Schematic diagram of the example.

Regulatory Guide 1.60 design-response spectrum, and the relationship between the two earthquakes must satisfy Abrahamson's seismic-motion-coherence function for a distance of 100 m. It is assumed that the behavior of a nuclear power plant is governed by horizontal earthquakes. One set of earthquakes consisted of two horizontal earthquakes (x-direction, y-direction). One set of earthquakes applied simultaneously in each direction on a single unit. Fig. 4 presents the generated input earthquakes in the same direction for each unit. Figs. 5 and 6 show the response spectra and seismic-motion-coherence functions of the two input earthquakes. A total of 30 sets of input earthquakes were generated. It can be seen that the two input earthquakes follow the target design-response spectrum of Regulatory Guide 1.60 and the seismic-motion-coherence function for a 100-m distance.

Fig. 7 shows the 120 generated response spectra and 60 coherence functions which is used to calculate the seismic response correlation coefficient. It can be seen that the mean curve of the generated input earthquake response spectrum exceeds the target response spectrum in Fig. 7(a). And the mean curve of the generated seismic motion coherency functions follows the trend of the target seismic motion coherency functions in Fig. 7 (b). It is lower than the target seismic motion coherency functions in the below 10 Hz and it is higher than the target seismic motion coherency functions in the above 10 Hz.

EDGs are assumed to be located within 100.5 ft of the auxiliary building at a standard Korean nuclear power plant. Therefore, the auxiliary-turbine/access-control-building complex was modeled for seismic-response analysis via the OpenSees finite-element-method program [24]. This building has a reinforced-concrete shear-wall structure and is connected to the turbine and access-control building. The lumped-stick model of this complex is shown in Fig. 8. The material properties used for probabilistic seismic analysis are given in Table 3.

Probabilistic seismic-response analysis was performed for the generated seismic motion and the generated structures. The damping ratio of the structure is kept at 4% by considering response level 1 of ASCE4-16, and soil-structure interactions were not considered [25]. Directional uncertainty is considered with a factor F_H, since the target-response spectrum is usually represented as a geometric mean. F_H is a lognormally distributed variable with a median value of 1.0 and a logarithmic standard deviation of 0.18 [25]. After F_H is generated, it is applied in the *x*-direction and $1/F_H$ is applied in the *y*-direction. For structural variability, the structural-stiffness and damping uncertainties are considered with a median value of 1.0 and logarithmic standard deviations of 0.30 and 0.35, respectively [25]. In addition, the correlation between the properties of the twin units was assumed to be independent.

The failure mode of EDG is anchor-concrete coning. The natural frequency of EDG is 36.4 Hz and its damping is 3%. The HCLPF of EDG is 0.38 g, the seismic-fragility curves are shown in Fig. 9, and the beta values are shown in Table 4. Fig. 10 shows the spectral-acceleration distribution at each EDG based on probabilistic seismic-response analysis.

Using Fig. 10 and Eq. (2), the EDG's seismic-response-correlation

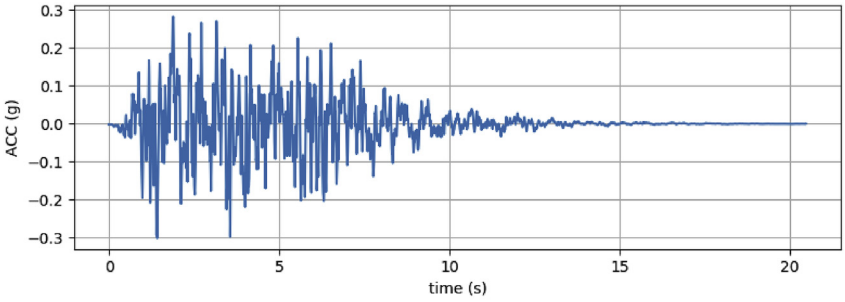

(a) seismic-input signal for A unit

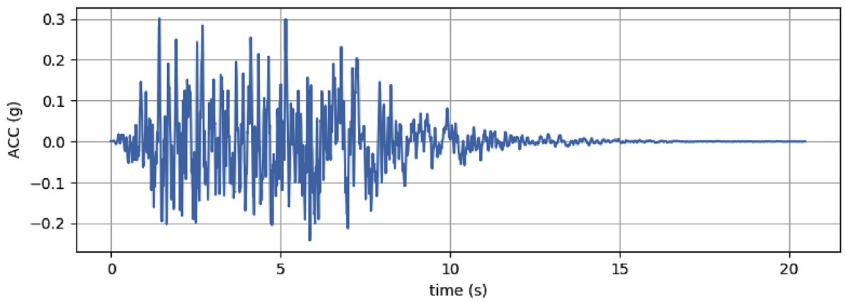

(b) seismic-input signal for B unit

Fig. 4. Seismic-input signals for the two units.

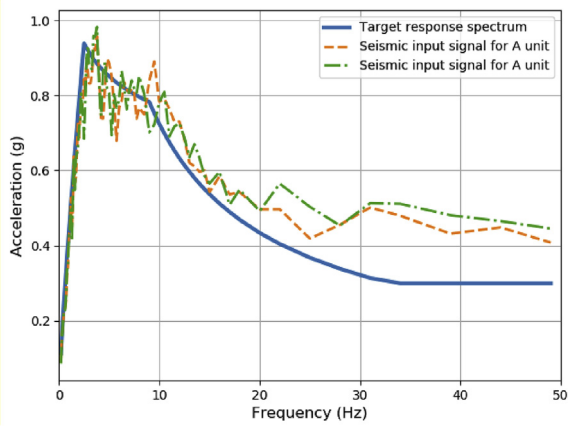

Fig. 5. Seismic-response spectra of the two seismic-input signals.

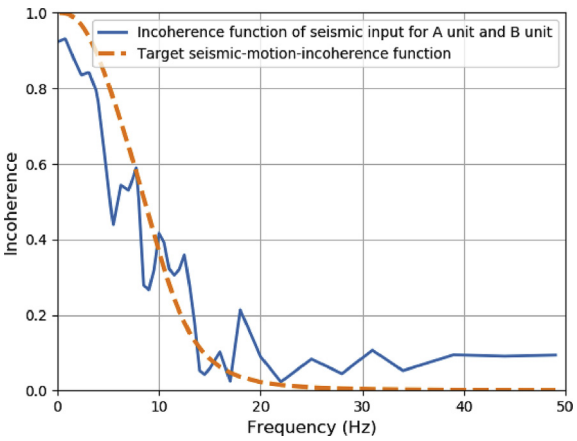

Fig. 6. Coherence function of two seismic-input signals for each unit.

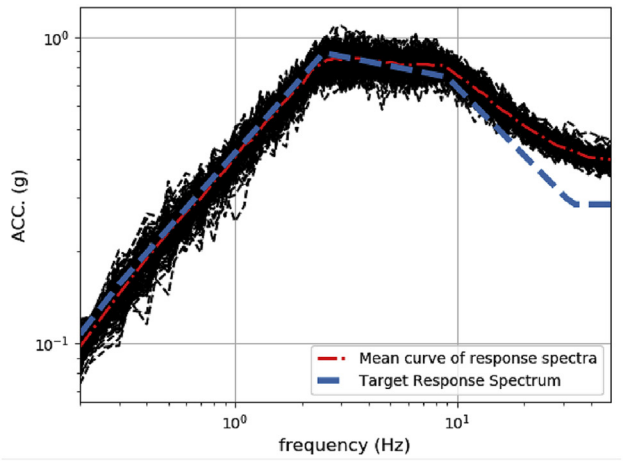

(a) Seismic-response spectra of generated seismic inputs

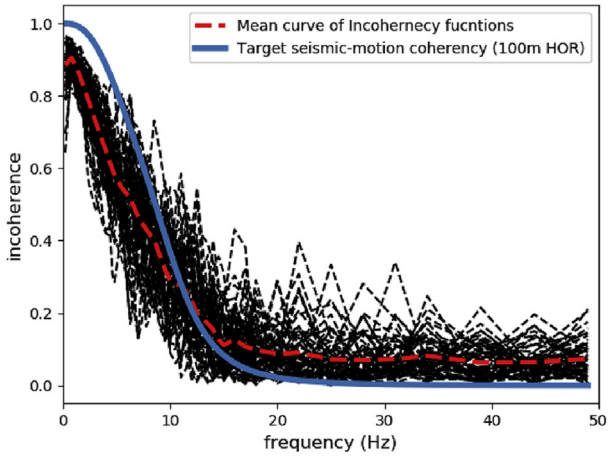

(b) Seismic motion coherency functions of generated seismic inputs

Fig. 7. Seismic-response spectra and seismic motion coherency functions of generated seismic-input signals.

coefficient is 0.3716. The seismic-failure-correlation coefficient between EDGs is required for seismic probabilistic safety assessment. The seismic-failure-correlation coefficient between EDGs can be obtained from the correlation coefficients for seismic response and seismic performance via Eq. (1). The seismic-capacity-correlation coefficient between EDGs should be obtained based on test results, and it is assumed to be either independent or fully dependent. Table 5 shows the standard deviations of the logarithms of the responses and of the capacities. Based on the above values, the seismic-failure-correlation coefficients for EDG are is shown in Table 6. The seismic-response and seismic-failure-correlation coefficients are adequately obtained using the proposed methodology for multi-unit risk (see Table 6).

4. Results and discussion

A method was proposed to calculate the seismic-response-correlation coefficient between SSCs using a seismic-motion-coherency function when the SSCs were located in different units in this study. The seismic-response and seismic-failure-correlation coefficients were calculated in this case using the above methodology.

In this chapter, the distribution of seismic-response-correlation coefficients is investigated according to the distance between SSCs. Distance was set to 100 m, 500 m, and 1000 m. The seismic-

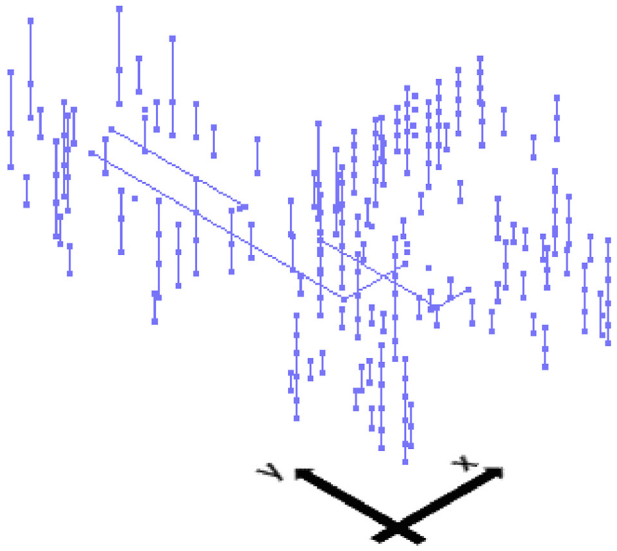

Fig. 8. Lumped-stick model of the auxiliary-turbine/access-control-building complex of the OPR1000 [24].

Table 3
Material properties of the structural model [24].

Material	Strength	Modulus of elasticity E	Shear modulus of elasticity G	Poisson's ratio ν	Weight density
Concrete	27.579 MPa	26,435 MPa	11,295 MPa	0.17	2403 kg/m^3
Structural Steel	344.738 MPa	199,948 MPa	79,979 MPa	0.27	7849 kg/m^3

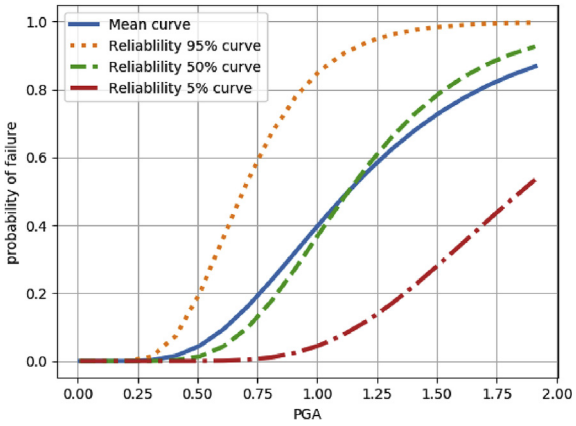

Fig. 9. Seismic-fragility curve of EDG.

Table 4
Beta values of EDG's fragility curve.

	β randomness	β uncertainty
Capacity Factor	0	0.17
Response Factor	0.24	0.08
Structure response Factor	0.27	0.24

Table 5
Beta values of EDGs for calculating the seismic-failure-correlation coefficient.

	Beta
standard deviations of the logarithms of the responses	0.44
standard deviations of the logarithms of the capacities	0.17

Table 6
Seismic-failure-correlation coefficient between EDGs.

	Seismic-failure-correlation coefficient
Assuming independent in seismic-capacity-correlation	0.323
Assuming fully dependent in seismic-capacity-correlation	0.453

Table 7
Floor elevations of the auxiliary building.

Slab No.	Identification	Elevation
1	Upper basement	23.470 m
2	Ground floor	30.632 m
3	Second floor	38.100 m
4	Third floor	43.891 m
5	Fourth floor	50.292 m
6	Roof	55.474 m

response-correlation coefficients of the SSCs were calculated by changing the frequency (5, 7.5, 10, 12.5, 15, 20, 50 Hz) and damping ratio (0.03 and 0.05), and they were assumed to be in the auxiliary buildings described in Table 7. The seismic-response-correlation-coefficient distribution is shown in Fig. 11 by a histogram and a gaussian kernel-density estimate.

The seismic-response-correlation-coefficient distribution of SSCs has two peaks and is distributed with a negative skewness, except when the SSCs are independent of each other. It can be seen from the distribution that the value is close to the independent condition is the highest. Moreover, the distribution differs depending on the distance; the negative-skewness value decreases as the distance between the two units increases, meaning that the seismic-response correlation between SSCs decreases.

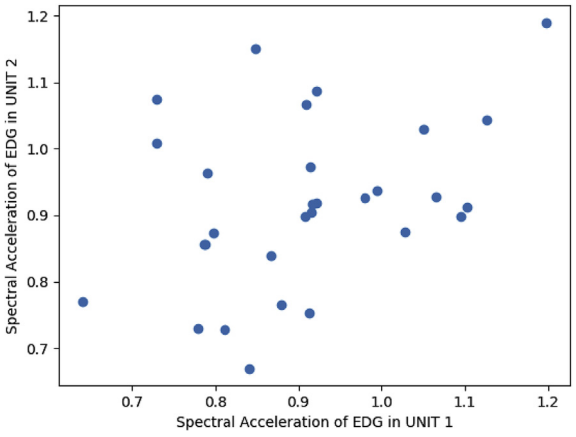

Fig. 10. Spectral-acceleration distribution of EDG.

The control point is not specified in this study. However, it is assumed that the same control point is used for two units by assuming the NPP site is on hard rock and the distance between two-units is close. Therefore, the same target response spectrum is used for two-units. When performing a seismic PSA for a site, its control point should not be defined for only a single unit. The seismic-hazard curve and the SSC's seismic-fragility curve should be defined for the control point of the site. The location of the control point affects the hazard curve of the site, the uniform hazard response spectrum, and the seismic fragility curve of the structure, system, and components. The seismic PSA for a multi-unit facility should be calculated from the same control point.

5. Conclusion

Multi-unit risk should be assessed to more accurately gage the possible accidents that may take place if several nuclear reactors are built at the same site. In addition, when evaluating the multi-unit seismic risk, it is necessary to perform risk evaluation considering the correlation between seismic failure between SSCs in each unit to obtain more reasonable results. Seismic-failure correlation exists between SSCs due to the characteristics of the earthquake and the seismic-risk value varies depending upon whether such correlation is considered.

One important factor for calculating seismic-failure correlation

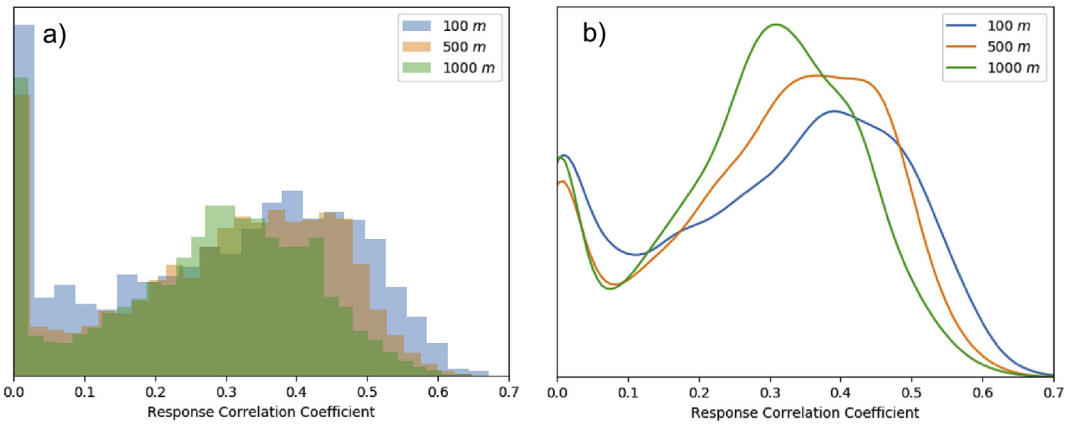

Fig. 11. (a) Histogram and (b) gaussian kernel-density estimate of the seismic-response-correlation-coefficient distribution due to the distance between two units.

is the seismic-response-correlation coefficient between SSCs. In this study, a method was proposed for obtaining the latter if there were multiple units on the site. For a seismic event, the input seismic signals at each location are similar due to having the same source, a similar path, and similar ground conditions. Therefore, to obtain the seismic-response-correlation coefficient between SSCs through seismic-response analysis, it is necessary to consider the similarity of the earthquakes applied to each structure.

We propose using the seismic-motion-coherence function to measure the similarity of this input earthquake. In other words, the seismic-motion-coherence function is used to determine the behavior of the earthquakes applied to seismic loads when performing probabilistic seismic-response analysis to calculate the risk to a nuclear power plant.

The seismic-response-correlation coefficients of EDGs located in auxiliary buildings at different locations were successfully derived using the proposed method. Those between EDGs were obtained assuming independent and fully dependent conditions of the seismic-capacity correlation. In addition, the distribution of the seismic-response-correlation coefficient was obtained as a function of distance for SSCs with various dynamic characteristics. The results showed that this distribution tended to decrease as the distance between the SSCs increased.

Declaration of competing interest

The authors declare that they have no known competing financial interests or personal relationships that could have appeared to influence the work reported in this paper.

Acknowledgements

This work was supported by the National Research Foundation of Korea (NRF) grant funded by the Korea government (MSIT) (No. 2020R1G1A1007570) and it was partially supported by Korea Hydro & Nuclear Power Co., Ltd. (No. L17S008002)

References

[1] M. Modarres, T. Zhou, M. Massoud, Advances in multi-unit nuclear power plant probabilistic risk assessment, Reliab. Eng. Syst. Saf. 157 (2017) 87–100.
[2] K. Ebisawa, et al., Concept and methodology for evaluating core damage frequency considering failure correlation at multi units and sites and its application, Nucl. Eng. Des. 288 (2015) 82–97.
[3] D.-S. Kim, et al., Multi-unit Level 1 probabilistic safety assessment: approaches and their application to a six-unit nuclear power plant site, Nuclear Eng. Technol. 50 (8) (2018) 1217–1233.
[4] D.-S. Kim, J.H. Park, H.-G. Lim, A pragmatic approach to modeling common cause failures in multi-unit PSA for nuclear power plant sites with a large number of units, Reliab. Eng. Syst. Saf. 195 (2020), 106739.
[5] C.S. Kumar, et al., Integrated risk assessment for multi-unit NPP sites—a comparison, Nucl. Eng. Des. 293 (2015) 53–62.
[6] S. Schroer, M. Modarres, An event classification schema for evaluating site risk in a multi-unit nuclear power plant probabilistic risk assessment, Reliab. Eng. Syst. Saf. 117 (2013) 40–51.
[7] J.-E. Yang, Multi-unit risk assessment of nuclear power plants: current status and issues, Nuclear Eng. Technol. 50 (8) (2018) 1199–1209.
[8] M. Ravindra, Sensitivity Studies of Seismic Risk Models, Electric Power Research Institute, Palo Alto, CA, 1984.
[9] U.S.N.R. Commission, Reactor Safety Study: an Assessment of Accident Risks in US Commercial Nuclear Power Plants, Nuclear Regulatory Commission, Washington, DC, 1975.
[10] R.J. Budnitz, Correlation of Seismic Performance in Similar SSCs (Structures, Systems, and Components), Nuclear Regulatory Commission, Washington, DC, 2017.
[11] S.-H. Eem, I.-K. Choi, Influence analysis of seismic risk due to the failure correlation in seismic probabilistic safety assessment, Journal of the Earthquake Engineering Society of Korea 23 (2) (2019) 101–108.
[12] P.D. Smith, et al., Seismic Safety Margins Research program.Phase I Final Report-Overview, Lawrence Livermore Laboratory, CA, 1981.
[13] M.P. Bohn, J.A. Lambright, Procedures For the External Event Core Damage Frequency Analyses for NUREG-1150, Nuclear Regulatory Commission, Washington, DC, 1990.
[14] M.P. Born, L.C. Shieh, J.E. Wells, Application of the SSMRP Methodology to the Seismic Risk at the Zion Nuclear Power Plant (NUREG/CR-3428), Nuclear Regulatory Commission, Washington, DC, 1983.
[15] N.A. Abrahamson, Program on Technology Innovation: Spatial Coherency Models for Soil-Structure Interaction, Electric Power Research Institute, Palo Alto, CA, 2006.
[16] N.A. Abrahamson, J.F. Schneider, J.C. Stepp, Empirical spatial coherency functions for application to soil-structure interaction analyses, Earthq. Spectra 7 (1) (1991) 1–27.
[17] R.S. Harichandran, E.H. Vanmarcke, Stochastic variation of earthquake ground motion in space and time, J. Eng. Mech. 112 (2) (1986) 154–174.
[18] E. Kausel, A. Pais, Stochastic deconvolution of earthquake motions, J. Eng. Mech. 113 (2) (1987) 266–277.
[19] C.-H. Loh, S.-G. Lin, Directionality and simulation in spatial variation of seismic waves, Eng. Struct. 12 (2) (1990) 134–143.
[20] C.H. Loh, Analysis of the spatial variation of seismic waves and ground movements from smart-1 array data, Earthq. Eng. Struct. Dynam. 13 (5) (1985) 561–581.
[21] P.G. Somerville, et al., Site-specific estimation of spatial incoherence of strong ground motion, Geotechnical Special Publication (n) (1988) 188–202.
[22] D. Zendagui, M.K. Berrah, E. Kausel, Stochastic deamplification of spatially varying seismic motions, Soil Dynam. Earthq. Eng. 18 (6) (1999) 409–421.
[23] S.A. Short, et al., Program on Technology Innovation: Effect of Seismic Wave Incoherence on Foundation and Building Response, Electric Power Research Institute, Palo Alto, 2006.
[24] S.-H. Eem, I.-K. Choi, Seismic response analysis of nuclear power plant structures and equipment due to the pohang earthquake, Journal of the Earthquake Engineering Society of Korea 22 (3) (2018) 113–119.
[25] A.S.o.C. Engineers, Seismic Analysis of Safety-Related Nuclear Structures and Commentary, American Society of Civil Engineers, 2016.